

# MR Fingerprinting for Rapid Quantitative Abdominal Imaging<sup>1</sup>

Yong Chen, PhD  
 Yun Jiang, BS  
 Shivani Pahwa, MD  
 Dan Ma, PhD  
 Lan Lu, PhD  
 Michael D. Twieg, MS  
 Katherine L. Wright, PhD  
 Nicole Seiberlich, PhD  
 Mark A. Griswold, PhD  
 Vikas Gulani, MD, PhD

## Purpose:

To develop a magnetic resonance (MR) “fingerprinting” technique for quantitative abdominal imaging.

## Materials and Methods:

This HIPAA-compliant study had institutional review board approval, and informed consent was obtained from all subjects. To achieve accurate quantification in the presence of marked  $B_0$  and  $B_1$  field inhomogeneities, the MR fingerprinting framework was extended by using a two-dimensional fast imaging with steady-state free precession, or FISP, acquisition and a Bloch-Siegert  $B_1$  mapping method. The accuracy of the proposed technique was validated by using agarose phantoms. Quantitative measurements were performed in eight asymptomatic subjects and in six patients with 20 focal liver lesions. A two-tailed Student  $t$  test was used to compare the T1 and T2 results in metastatic adenocarcinoma with those in surrounding liver parenchyma and healthy subjects.

## Results:

Phantom experiments showed good agreement with standard methods in T1 and T2 after  $B_1$  correction. In vivo studies demonstrated that quantitative T1, T2, and  $B_1$  maps can be acquired within a breath hold of approximately 19 seconds. T1 and T2 measurements were compatible with those in the literature. Representative values included the following: liver, 745 msec  $\pm$  65 (standard deviation) and 31 msec  $\pm$  6; renal medulla, 1702 msec  $\pm$  205 and 60 msec  $\pm$  21; renal cortex, 1314 msec  $\pm$  77 and 47 msec  $\pm$  10; spleen, 1232 msec  $\pm$  92 and 60 msec  $\pm$  19; skeletal muscle, 1100 msec  $\pm$  59 and 44 msec  $\pm$  9; and fat, 253 msec  $\pm$  42 and 77 msec  $\pm$  16, respectively. T1 and T2 in metastatic adenocarcinoma were 1673 msec  $\pm$  331 and 43 msec  $\pm$  13, respectively, significantly different from surrounding liver parenchyma relaxation times of 840 msec  $\pm$  113 and 28 msec  $\pm$  3 ( $P < .0001$  and  $P < .01$ ) and those in hepatic parenchyma in healthy volunteers (745 msec  $\pm$  65 and 31 msec  $\pm$  6,  $P < .0001$  and  $P = .021$ , respectively).

## Conclusion:

A rapid technique for quantitative abdominal imaging was developed that allows simultaneous quantification of multiple tissue properties within one 19-second breath hold, with measurements comparable to those in published literature.

©RSNA, 2016

<sup>1</sup>From the Departments of Radiology (Y.C., S.P., D.M., L.L., K.L.W., M.A.G., V.G.), Biomedical Engineering (Y.J., N.S., M.A.G.), and Electrical Engineering and Computer Science (M.D.T.), Case Western Reserve University/University Hospitals Case Medical Center, 11100 Euclid Ave, Bolwell Building, Room B120, Cleveland, OH 44106. Received September 15, 2015; revision requested October 29; revision received November 6; accepted December 7; final version accepted December 11. Supported by Siemens Healthcare. Address correspondence to V.G. (e-mail: [vxg46@case.edu](mailto:vxg46@case.edu)).

©RSNA, 2016

**M**agnetic resonance (MR) imaging is traditionally qualitative, and underlying tissue properties, especially the relaxation times T1 and T2, which affect the signal of every MR image, are rarely measured. However, when they are obtained, quantitative measurements have the potential for usefulness in multiple clinical scenarios, such as differentiating cirrhotic from noncirrhotic liver (1), providing surrogate markers of function in native and transplanted kidneys (2), hepatic lesion characterization (3–5), and assessment of response to treatment (6,7). However, quantitative MR imaging is often an inefficient process, because multiple weighted images are needed to generate a single map, and can be extremely challenging in moving regions, such as the abdomen. Presently, in most clinical scenarios, it is not time efficient to map a physical property rather than

examine a single image weighted by that property. The need for quantitative property mapping must be proven for each clinical scenario, and this can also be challenging because of acquisition time constraints.

Recently, a new approach, namely, MR “fingerprinting,” was introduced to simultaneously measure several important properties in a single examination (8). MR fingerprinting uses an acquisition in which imaging unit settings are allowed to vary greatly in a seemingly random manner to generate incoherent magnetization signals. To process these signals, Bloch simulations are first used to generate a dictionary of signal evolutions from all possible property values. A template-matching algorithm is then applied to identify the closest signal evolution for each pixel, thereby yielding the property values for the pixel. Work in the brain has shown that accurate quantification of proton density ( $M_0$ ) and T1 and T2 relaxation times can be achieved in less than 10 seconds, which opens the door to rapid quantitative analysis of pathologic conditions in a multiproperty space (9).

Although it has shown great promise in stationary brain imaging, quantitative parameter measurement in the abdomen is even more challenging. In extending the MR fingerprinting technique from brain to abdominal imaging, physiologic motion is a major concern, and an efficient measurement that can be completed within a clinically feasible breath hold is needed. Second, achieving sufficient spatial resolution to detect small lesions is challenging in abdominal imaging, as very large fields of view (FOVs) (40–50 cm) are needed for coverage of large

or spatially diffuse organs such as the liver and bowel. Finally, because of the large FOV requirements, substantial challenges for quantitative imaging are expected from both static ( $B_0$ ) and transmit ( $B_1$ ) magnetic field inhomogeneities, which are particularly problematic at high field strengths (3.0 T and beyond). The goal of this study was to develop an MR fingerprinting technique for quantitative abdominal imaging.

### Advances in Knowledge

- A quantitative abdominal imaging technique based on the MR fingerprinting framework is introduced.
- Despite the presence of  $B_1$  inhomogeneities, simultaneous quantification of T1 and T2 in the abdomen can be achieved within one breath hold of approximately 19 seconds (key mean tissue T1 and T2 measurements, respectively, were as follows: liver, 745 msec  $\pm$  65 [standard deviation] and 31 msec  $\pm$  6; renal medulla, 1702 msec  $\pm$  205 and 60 msec  $\pm$  21; renal cortex, 1314 msec  $\pm$  77 and 47 msec  $\pm$  10; spleen, 1232 msec  $\pm$  92 and 60 msec  $\pm$  19; skeletal muscle, 1100 msec  $\pm$  59 and 44 msec  $\pm$  9; and fat, 253 msec  $\pm$  42 and 77 msec  $\pm$  16).
- T1 and T2 in metastatic adenocarcinoma were found to be 1673 msec  $\pm$  331 and 43 msec  $\pm$  13, respectively—significantly higher than those in surrounding liver parenchyma (T1, 840 msec  $\pm$  113; T2, 28 msec  $\pm$  3;  $P < .0001$  and  $P < .01$ , respectively).




### Implications for Patient Care

- The technology of MR fingerprinting can be extended to abdominal imaging.
- Relaxation times can be simultaneously mapped and applied for characterization of focal abdominal lesions or diffuse parenchymal diseases.

### Materials and Methods

The authors receive research grant support from Siemens Healthcare (Erlangen, Germany). They hold patents for MR fingerprinting technology, which has been licensed by Siemens. The authors had full control of the research and all data presented here, and no influence on the content was exerted by Siemens Healthcare. This prospective study was approved by the institutional review board and was compliant with the Health Insurance Portability and Accountability Act. Informed written consent was obtained

### Published online before print

10.1148/radiol.2016152037 Content codes:   

Radiology 2016; 279:278–286

### Abbreviations:

FISP = fast imaging with steady-state free precession  
FOV = field of view

### Author contributions:

Guarantors of integrity of entire study, Y.C., M.D.T., M.A.G., V.G.; study concepts/study design or data acquisition or data analysis/interpretation, all authors; manuscript drafting or manuscript revision for important intellectual content, all authors; manuscript final version approval, all authors; agrees to ensure any questions related to the work are appropriately resolved, all authors; literature research, Y.C., Y.J., S.P., K.L.W., V.G.; clinical studies, Y.C., S.P., V.G.; experimental studies, Y.C., Y.J., D.M., L.L., M.D.T., K.L.W., N.S., V.G.; statistical analysis, Y.C., V.G.; and manuscript editing, Y.C., Y.J., S.P., M.D.T., K.L.W., N.S., M.A.G., V.G.

### Funding:

This research was supported by the National Institutes of Health (grants 1R01DK098503, 1R01EB017219, 5R01EB016728, R00EB011527, and 2KL2TR000440).

Conflicts of interest are listed at the end of this article.

from all volunteers before the MR imaging examinations.

### Data Acquisition for Abdominal MR Fingerprinting

MR imaging experiments were performed with a 3.0-T imaging unit (Skyra; Siemens Healthcare). The original MR fingerprinting acquisition proposed for brain imaging was based on an inversion-recovery balanced steady-state free precession (bSSFP) pulse sequence. However, magnetic field inhomogeneities are a major problem for bSSFP-based sequences for abdominal MR imaging at 3.0 T. Thus, an alternative MR fingerprinting method based on another steady-state sequence, namely, fast imaging with steady-state free precession (FISP), was used (10). For FISP MR fingerprinting, an adiabatic inversion pulse was applied first, followed by a FISP data acquisition with pseudorandomized repetition times and flip angles (Fig 1, A and B) (8,10). Although 82 914 possible signal time courses are in the MR fingerprinting dictionary, several simulated signal evolution curves from five abdominal tissues (based on known T1 and T2 for these tissues) are shown in Figure 1, C. Because these tissues have different characteristic T1 and T2 values (11), different signal evolution patterns were observed, which provided the basis for using the MR fingerprinting algorithm to differentiate various tissue types in the abdomen.

To accelerate data sampling, highly undersampled images were acquired with a fast spiral readout. With the minimum-time gradient design method, 48 spiral interleaves with zero moment gradient compensation were designed for a two-dimensional image to meet the Nyquist criteria. The maximum gradient amplitude and slew rate were 21 mT/m and 162 mT/m/msec, respectively. To achieve a fast signal readout for the enlarged FOV of abdominal imaging, a uniform-density spiral trajectory was used instead of the variable-density spiral trajectory introduced in the original MR fingerprinting method (8). With

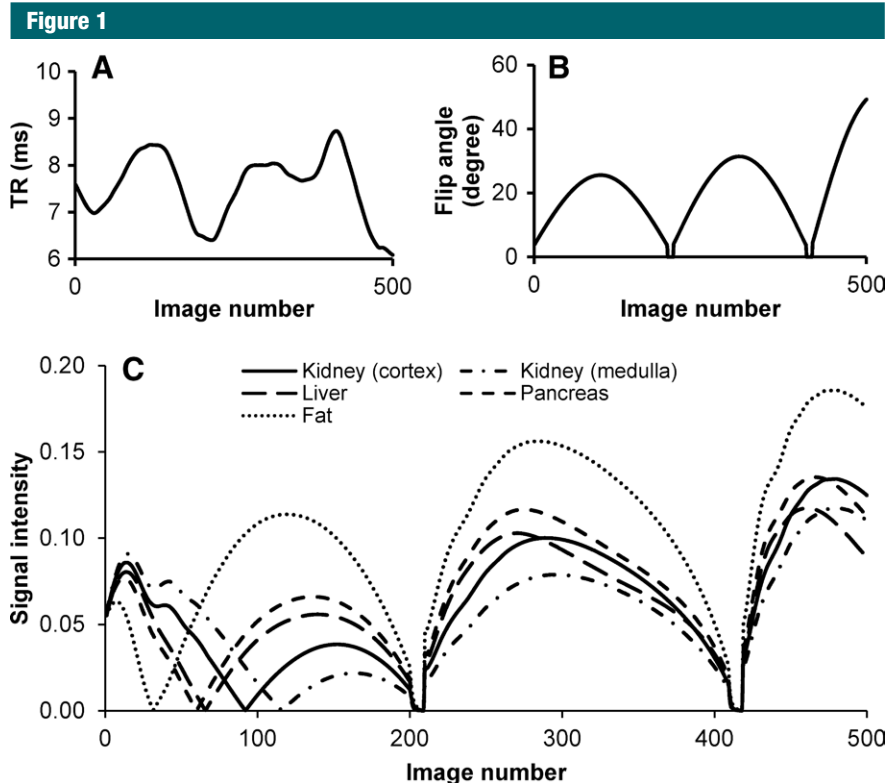


**Figure 1:** A–C, Simulation of signal evolution curves for FISP MR fingerprinting. A, B, Example of first 500 points of repetition time (*TR*) and flip angle patterns. C, Signal evolution curves for multiple tissues in the abdomen created by using the patterns in A and B. T1 and T2 values, respectively, used to generate the curves included 1140 and 75 msec for the renal cortex, 1540 and 80 msec for the renal medulla, 820 and 35 msec for the liver, 720 and 45 msec for the pancreas, and 400 and 70 msec for fat (11).

the same spatial coverage (44 cm) and resolution (2 mm), the readout time was reduced from 6.2 to 2.9 msec for each spiral interleaf. The designed trajectory was measured by using the method proposed by Duyn et al (12) with a doped water phantom. For FISP MR fingerprinting, only one spiral interleaf was actually used to generate each image (acceleration factor, 48), which resulted in highly aliased images. A total of 2500 spiral arms, and thus 2500 undersampled images, were acquired in 17 seconds; the spiral interleaf in each image was rotated 7.5° to provide different spatial encoding. Other imaging parameters were as follows: FOV, 44 × 44 cm; matrix size, 224 × 224 (for an effective in-plane resolution of 1.9 mm); echo time, 1.3 msec; section thickness, 5 mm (single-section two-dimensional acquisition);

and radiofrequency pulse, 1-msec sinc pulse (time-bandwidth product, 4).

A major concern in the application of FISP MR fingerprinting for high-field-strength abdominal imaging is the transmit field ( $B_1$ ) inhomogeneities encountered over the large FOV. In this study, a transmit field ( $B_1$ ) map was acquired by using the Bloch-Siegert technique within the same breath hold used for the FISP MR fingerprinting acquisition (13). For fast imaging purposes and for the reduction of specific absorption rate, a gradient-echo-based Bloch-Siegert sequence was implemented with a multi-shot spiral acquisition (24 spiral interleaves for each image). Two images were acquired with  $\pm 4$  kHz frequency off-resonance in an interleaved manner; the total acquisition time for a  $B_1$  map was 1.8 seconds.

Table 1

**Ranges and Step Sizes for T<sub>1</sub>, T<sub>2</sub>, and B<sub>1</sub> in the Dictionary**

Parameter and Range	Step Size
<b>T<sub>1</sub> (msec)</b>	
100–600	100
600–1600	20
1700–2200	100
2300–3000	300
<b>T<sub>2</sub> (msec)</b>	
5–100	5
110–200	10
300–500	100
<b>B<sub>1</sub> (unitless)</b>	
0.1–2	0.05

**Image Reconstruction and Processing**

Image reconstruction and postprocessing were performed offline in Matlab (Mathworks, Natick, Mass). To retrieve tissue properties (T<sub>1</sub>, T<sub>2</sub>, and M<sub>0</sub>) from the FISP MR fingerprinting experiment, a dictionary that included the signal evolutions from all possible combinations of parameters for a T<sub>1</sub> range of 100–3000 msec, a T<sub>2</sub> range of 5–500 msec, and a B<sub>1</sub> range of 10%–200% of the nominal value was calculated by using Bloch simulations (14). B<sub>1</sub> was simulated as a ratio of obtained flip angle divided by the nominal (expected) flip angle and thus was unitless. A perfect agreement between obtained and expected flip angle would be expected to give a ratio of 1.

The detailed ranges and step sizes used for T<sub>1</sub>, T<sub>2</sub>, and B<sub>1</sub> in the calculation are presented in Table 1. Step sizes are defined as the incremental changes in T<sub>1</sub>, T<sub>2</sub>, or B<sub>1</sub> between adjacent entries in the simulated dictionary. The acquired signal in each pixel of highly accelerated images was then matched to those entries in the dictionary that had the same B<sub>1</sub> values as measured (Fig 2). One best entry was identified by using the same method used in the original MR fingerprinting implementation (8), which in turn yielded all underlying parameters that were used to form the dictionary entry. The original MR fingerprinting reconstruction

Figure 2

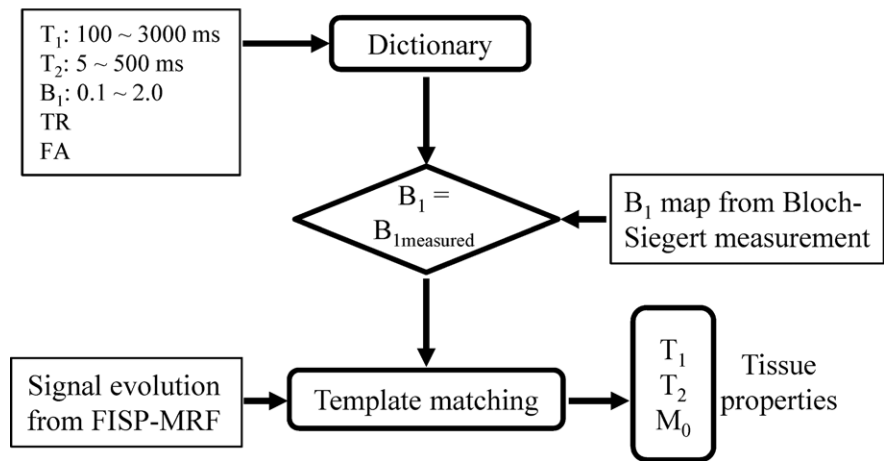


**Figure 2:** Diagram for the FISP MR fingerprinting (MRF) analysis with the inclusion of B<sub>1</sub> correction. FA = flip angle, TR = repetition time.

without the B<sub>1</sub> correction (assuming a uniform B<sub>1</sub> map of 1) was also performed as a comparison. The calculation time for parameter mapping of one section was about 3 minutes with a standard desktop computer (Xeon E3–1270 quad-core central processing units at 3.4 GHz and 16 GB of random-access memory; Intel, Santa Clara, Calif).

**Phantom Studies**

The accuracy of the FISP MR fingerprinting method was first validated by using an agarose gel phantom. Because phantom experiments typically have a uniform transmit B<sub>1</sub> field, a tuned transmit surface coil passively coupled to the body coil was used for the FISP MR fingerprinting measurement to purposely generate a nonuniform B<sub>1</sub> field. T<sub>1</sub> and T<sub>2</sub> relaxation times obtained from the FISP MR fingerprinting measurements (with or without consideration of the induced B<sub>1</sub> field) were then compared with reference T<sub>1</sub> and T<sub>2</sub> values obtained by using standard single-echo spin-echo sequences. Reference T<sub>1</sub> values were established by using an inversion-recovery single-echo spin-echo sequence with a repetition time of 6 seconds and seven inversion times from 50 to 3800 msec. Reference T<sub>2</sub> values were measured by using a single-echo spin-echo sequence with a repetition

time of 6 seconds and eight echo times from 20 to 800 msec.

**In Vivo Studies**

After phantom validation, quantitative measurements with FISP MR fingerprinting were obtained in eight asymptomatic subjects (three men [mean age, 22 years; range, 19–23 years] and five women [mean age, 25 years; range, 19–43 years]) and six patients (four men [mean age, 60 years; range, 53–69 years] and two women [mean age, 58 years; range, 46–69 years]) with metastatic adenocarcinoma and a total of 20 lesions. For each asymptomatic subject, the FISP MR fingerprinting and B<sub>1</sub> measurements were performed at one to three different section locations in the axial orientation. For each section, the two acquisitions (FISP MR fingerprinting and B<sub>1</sub>) were performed consecutively in a single breath hold of approximately 19 seconds to ensure the same section coverage. For the examinations in patients, the sections were prescribed at the location of liver lesions on coronal T<sub>2</sub>-weighted images or on the basis of findings at previous MR imaging studies.

**Statistical Analysis**

A two-tailed Student *t* test was used to compare the T<sub>1</sub> and T<sub>2</sub> results obtained in eight healthy subjects and in

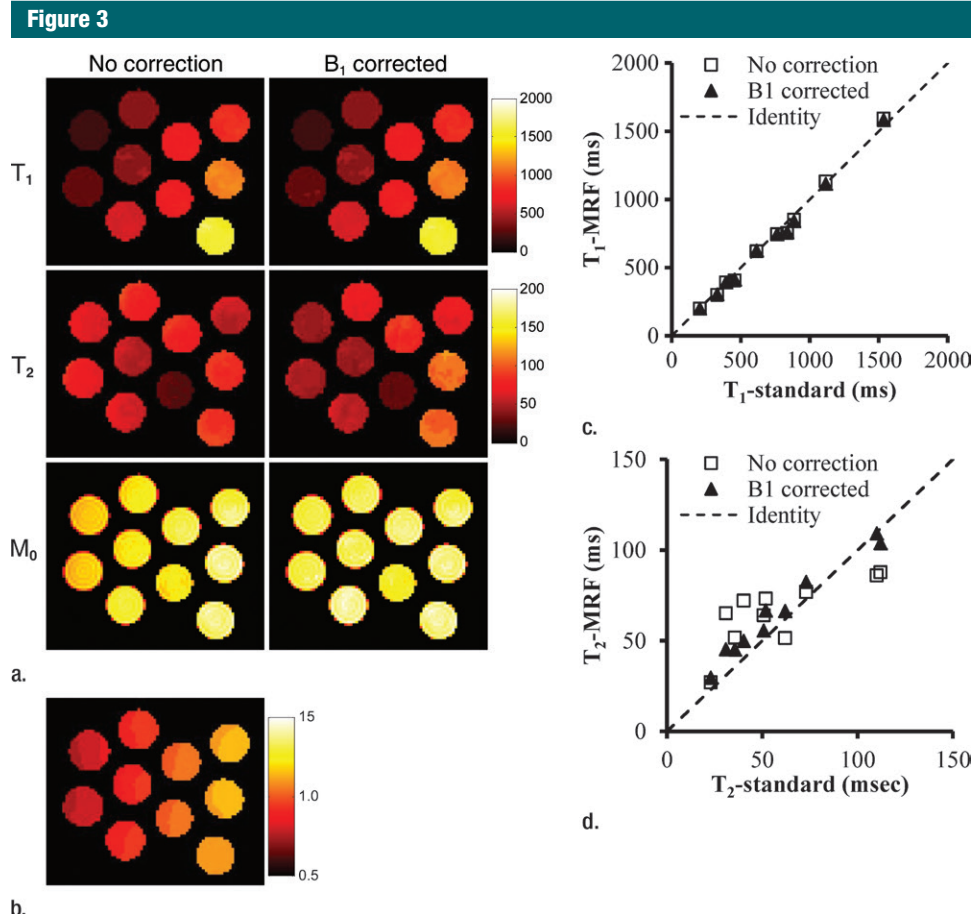


**Figure 3:** (a) Phantom T<sub>1</sub>, T<sub>2</sub>, and proton density (M<sub>0</sub>) maps acquired by using the FISP MR fingerprinting method before and after B<sub>1</sub> correction. (b) B<sub>1</sub> map for the phantoms. Although a close match in the T<sub>1</sub> maps was observed before and after B<sub>1</sub> correction, substantial changes in the T<sub>2</sub> map were noticed after B<sub>1</sub> correction. (c, d) Graphs show comparison of T<sub>1</sub> (c) and T<sub>2</sub> (d) values obtained with the FISP MR fingerprinting method and those obtained with the reference method.

six patients with metastatic adenocarcinoma. Normal distributions for each population and each relaxation property were verified.  $P < .05$  was considered to indicate a significant difference.

## Results

Figure 3 presents the T<sub>1</sub>, T<sub>2</sub>, and proton density maps acquired in phantom studies in which the FISP MR fingerprinting method was used before and after B<sub>1</sub> correction. With the additional surface coil-induced transmit inhomogeneity, a maximum of 45% change in B<sub>1</sub> magnitude was observed, which is similar in scale to the B<sub>1</sub> variation observed in in vivo abdominal

measurements (15,16). Unlike conventional methods, which typically show a dependence of T<sub>1</sub> on B<sub>1</sub>, our phantom results consistently showed a dependence of T<sub>2</sub> on B<sub>1</sub> without correction. However, after B<sub>1</sub> correction, both T<sub>1</sub> and T<sub>2</sub> values were in improved agreement with values acquired by using the reference-standard measurement. The average T<sub>2</sub> deviations from the reference standard were 18.4 msec  $\pm$  10.6 (range, 4.0–34.3 msec) before correction and 8.3 msec  $\pm$  4.4 (range, 0.8–15.0 msec) after correction.

Figure 4, A shows a representative image from 2500 images in a healthy volunteer. As expected, substantial aliasing artifacts are present because of

the high acceleration factor of 48 for each image in the FISP MR fingerprinting acquisition. The corresponding B<sub>1</sub> map for this section is shown in Figure 4, B. The three quantitative maps (T<sub>1</sub>, T<sub>2</sub>, and M<sub>0</sub>) obtained before and after B<sub>1</sub> correction are shown in Figure 4, C–H, and the difference maps between them are shown in Figure 4, I–K. As in the phantom experiment, a more pronounced difference was seen in the T<sub>2</sub> map (compared with the T<sub>1</sub> map) after B<sub>1</sub> correction, and the pattern of T<sub>2</sub> difference matched well with that of the B<sub>1</sub> map (Fig 4, B and J). Compared with the T<sub>2</sub> map without B<sub>1</sub> correction (Fig 4, D), a smoother T<sub>2</sub> map was observed in the whole liver after B<sub>1</sub>

Figure 4

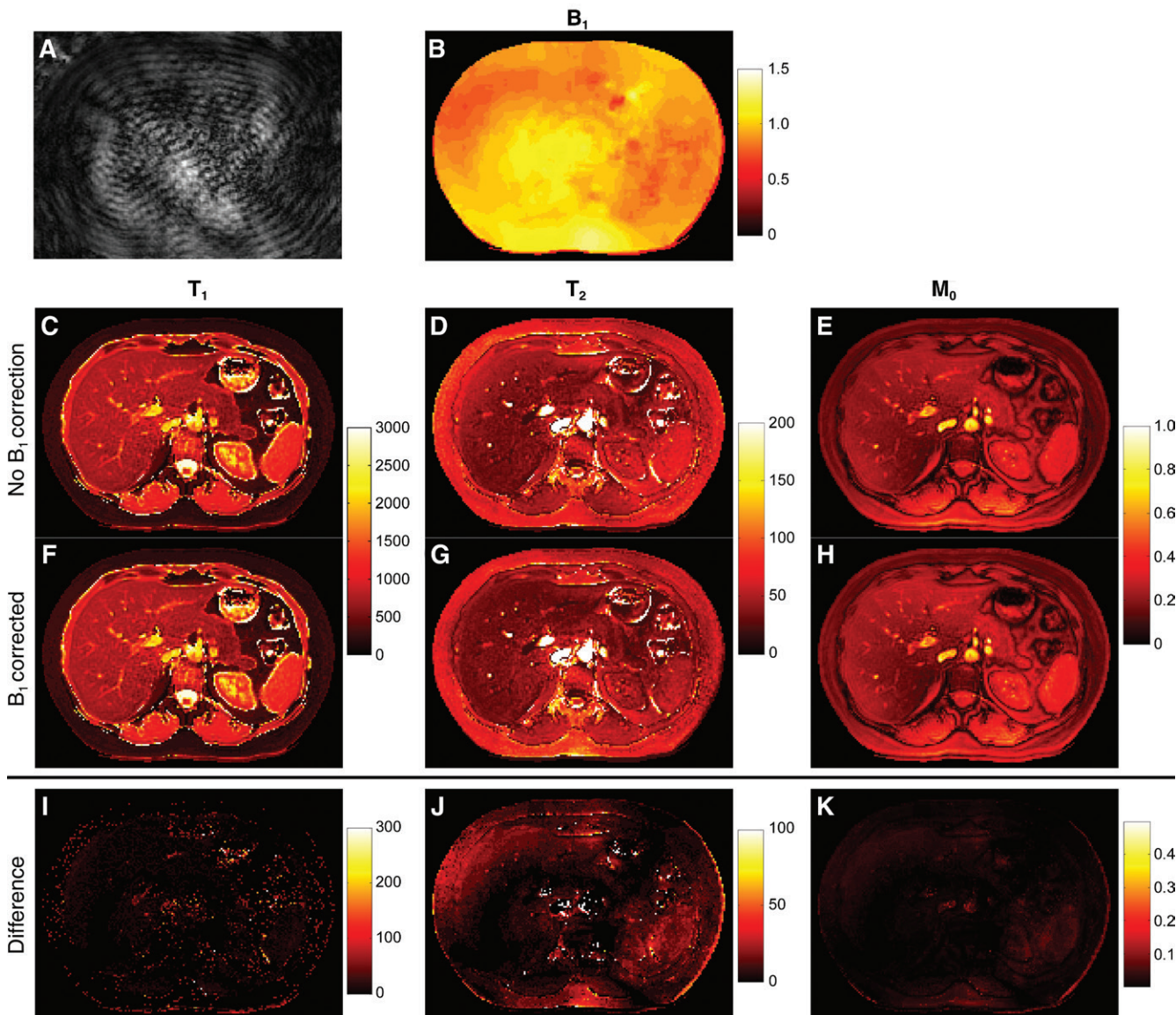


**Figure 4:** A–K, Representative quantitative maps (T<sub>1</sub>, T<sub>2</sub>, M<sub>0</sub>) acquired in a healthy subject. A, A representative highly undersampled image shows marked aliasing artifacts (acceleration factor for each image, 48). B, B<sub>1</sub> map. C–E, Quantitative maps (T<sub>1</sub>, T<sub>2</sub>, and M<sub>0</sub>) obtained without B<sub>1</sub> correction. F–H, Quantitative maps obtained with B<sub>1</sub> correction. I–K, Difference maps. A clear difference in the T<sub>2</sub> map rather than the T<sub>1</sub> map was observed after B<sub>1</sub> correction, and the pattern of T<sub>2</sub> difference matches well with that of the B<sub>1</sub> map (in B).

correction (Fig 4, G). Average T<sub>1</sub> and T<sub>2</sub> values of multiple abdominal organs acquired in the eight healthy subjects are presented in Table 2.

Figure 5 shows the quantitative MR fingerprinting maps and several conventional images acquired in a patient with metastatic lung adenocarcinoma. Two metastatic lesions (lesion 1, 33

mm; lesion 2, 10 mm) were observed in the liver on the basis of the quantitative MR fingerprinting results (Fig 5, D and E) corresponding to the lesions seen on the clinical computed tomographic (CT) and MR images (Fig 5, A and B). Compared with relaxation times in the healthy surrounding tissue, longer T<sub>1</sub> relaxation times were observed for

both metastatic lesions (lesion 1, 1462 msec; lesion 2, 1582 msec; surrounding tissue, 686 msec). Longer T<sub>2</sub> was observed only in lesion 1, and not in lesion 2, as compared with the surrounding tissue (lesion 1, 57 msec; lesion 2, 19 msec; surrounding tissue, 26 msec). The mean T<sub>1</sub> and T<sub>2</sub> relaxation times in all 20 lesions in the six patients with

Table 2

## Average T1 and T2 Relaxation Times of Abdominal Tissues Acquired in Healthy Subjects at 3.0 T

Tissue	T1 (msec)		T2 (msec)	
	This Study	Literature	This Study	Literature
Liver*	745 ± 65	809 ± 71 (11)	31 ± 6	34 ± 4 (11)
		824 ± 61 (17)		42 ± 3 (18)
		812 ± 64 (18)		
Kidney medulla	1702 ± 205	1545 ± 142 (11)	60 ± 21	81 ± 8 (11)
		1610 ± 55 (17)		
Kidney cortex	1314 ± 77	1142 ± 154 (11)	47 ± 10	76 ± 7 (11)
		1194 ± 88 (17)		
Spleen	1232 ± 92	1328 ± 31 (11)	60 ± 19	61 ± 9 (11)
		1251 ± 95 (17)		
Skeletal muscle	1100 ± 59	898 ± 33 (11)	44 ± 9	29 ± 4 (11)
		1017 ± 78 (17)		50 ± 4 (18)
		1412 ± 13 (18)		
Fat	253 ± 42	343 ± 37 (11)	77 ± 16	68 ± 4 (11)
		307 ± 37 (17)		

Note.—Data are means ± standard deviations.

\* The liver T1 and T2 relaxation times were compared with patient data.

metastatic adenocarcinoma were 1673 msec ± 331 and 43 msec ± 13, respectively—significantly higher than those in the surrounding liver parenchyma (T1, msec 840 ± 113 [ $P < .0001$ ]; T2, 28 msec ± 3 [ $P < .01$ ]) and in asymptomatic volunteers (Table 2) ( $P < .0001$  for T1 and  $P = .021$  for T2).

## Discussion

A variety of fast imaging techniques have been proposed for quantification of T1 and T2 relaxation times. However, most of the technologies focus on imaging stationary brain tissues. This work demonstrates simultaneous measurement of multiple physical properties for abdominal imaging. All property maps are coregistered, which aids in creating a multiproperty quantitative space for lesion characterization.

$B_1$  inhomogeneity is a well-known problem in 3.0 T imaging and is thus expected to affect the accuracy of relaxation property mapping (15,16,19). While it is less of an issue for MR fingerprinting studies with brain imaging at 1.5 T or 3.0 T, it is well known that large variation in  $B_1$  is expected with abdominal imaging at 3.0 T because of the

large FOV and increased dielectric effects. Thus, this issue must be accounted for in abdominal MR fingerprinting. In this study, we adopted the Bloch-Siegert technique, which has been shown to provide accurate and efficient  $B_1$  mapping that is insensitive to T1 and  $B_0$  field inhomogeneities (13). We further improved the efficiency of this technique by combining it with a fast spiral readout. The improved method provides a 12-fold acceleration in imaging time while preserving similar spatial resolution. Although the proposed technique was developed and validated at 3.0 T for the abdomen, the degree of  $B_1$  inhomogeneities encountered were similar to those encountered in the brain at 7.0 T. The proposed technique provides a method for measurements in the setting of severe  $B_1$  field inhomogeneities, adding to approaches such as parallel transmission (20).

An interesting finding in both our phantom and in vivo studies is that, unlike conventional methods, which typically show a dependence of T1 on the  $B_1$ , the proposed FISP MR fingerprinting technique consistently exhibits a dependence of T2 on  $B_1$ . This difference is likely due to the distinct T1

encoding algorithms used in the FISP MR fingerprinting technique. Most conventional T1 mapping methods, such as the variable flip angle method and the Look-Locker method (16,17), typically use either an inversion pulse or varying flip angles or repetition times as the only mechanism to encode T1 weighting. With FISP MR fingerprinting, the inversion pulse applied before the FISP readout train, as well as variable flip angles and repetition times, all contribute to impart T1 weighting, which results in a robust T1 quantification that is independent of  $B_1$ .

The initial demonstration of the technique in six patients with focal liver lesions demonstrated that the method can provide localized quantitative information in settings of disease. The longer T1 and T2 relaxation times in metastatic lesions are consistent with previous clinical and preclinical findings (5,21,22). Recent studies have also investigated the possibility of using relaxation times to predict tumor response to treatment. Although T2 does not appear to be an early indicator of response (22), T1 does appear to be a promising indicator for predicting response to chemotherapy (6,7). Simultaneous mapping of properties also allows the creation of a multiproperty space to characterize pathologic conditions. The proposed FISP MR fingerprinting technique provides an ideal option for this type of analysis. The present patient examples offer a proof of concept, and studies with larger numbers of patients with different lesion types will be needed for more detailed comparisons with results in published literature and for application in open clinical questions, such as more definitive lesion characterization and monitoring response to therapy.

One limitation of the proposed method is two-dimensional acquisition, as extension to three-dimensional acquisition is still restricted by imaging speed. Further work combining this technology with acceleration techniques such as parallel imaging, iterative reconstruction, and multiband excitation is needed to facilitate volumetric

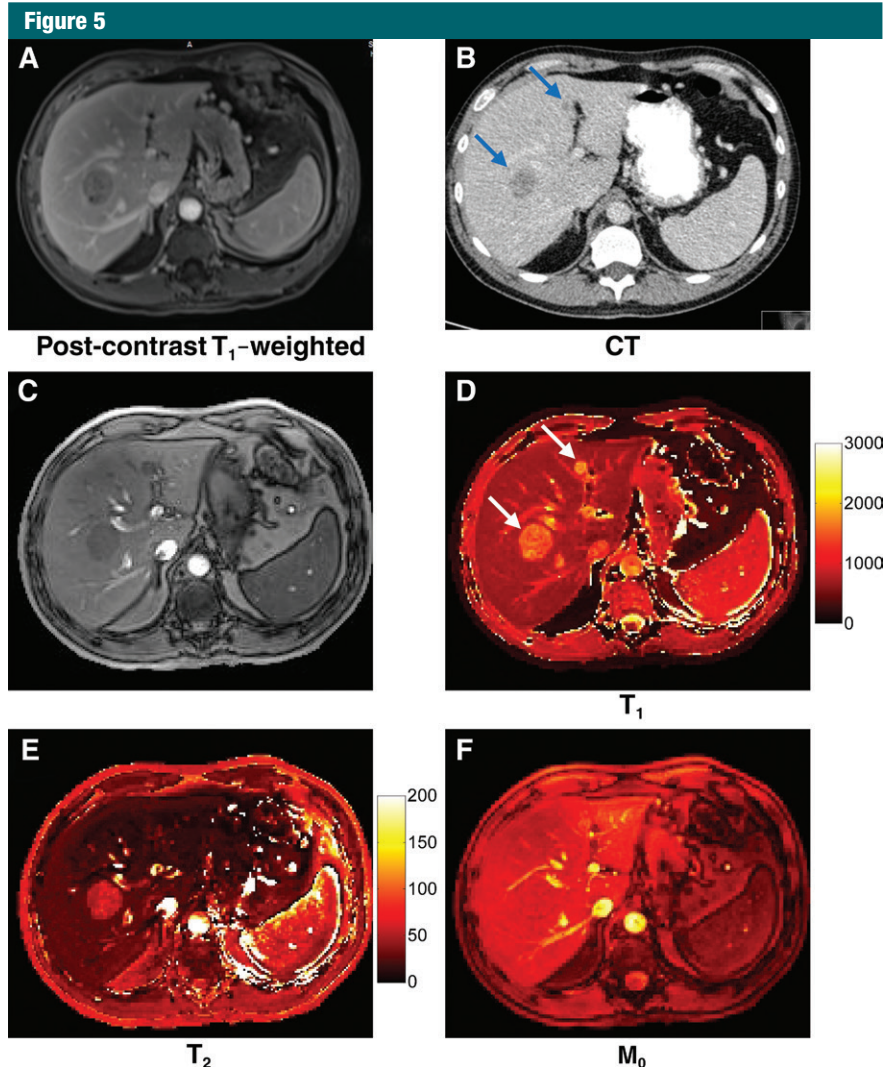


**Figure 5:** Images acquired in a patient with lung adenocarcinoma metastatic to the liver. *A*, Conventional contrast material-enhanced  $T_1$ -weighted MR image (three-dimensional fat-saturated gradient-echo; repetition time msec/echo time msec, 4.34/1.84; flip angle,  $13^\circ$ ; FOV,  $440 \times 282$  mm; matrix,  $224 \times 146$ ; section thickness, 3 mm). *B*, CT image. *C*, Image summed from all undersampled images. *D–F*, Quantitative  $T_1$ ,  $T_2$ , and  $M_0$  maps. Two metastatic lesions measuring 33 and 10 mm in diameter (arrows) on the  $T_1$  map were seen on both conventional images and quantitative maps.

coverage within a breath hold (23–25). Finally, validation experiments were conducted in phantoms and not in patients. Reference-standard long-spin-echo experiments would require breath holds that could not be provided by patients.

Further work also continues to expand the MR fingerprinting framework for obtaining measurements of other tissue properties, in addition to relaxation times. MR fingerprinting has been

successfully used to obtain dynamic susceptibility contrast-enhanced perfusion images in the brain (26). Preliminary studies for obtaining diffusion and perfusion measurements simultaneously with relaxation property measurements have been reported (27,28).

In conclusion, a rapid technique for quantitative abdominal imaging was developed by using an FISP MR fingerprinting acquisition in combination with the Bloch-Siebert  $B_1$  mapping method,

allowing simultaneous quantification of  $T_1$  and  $T_2$  in the abdomen within a 19-second breath hold.

**Disclosures of Conflicts of Interest:** **Y.C.** Activities related to the present article: received a grant from Siemens Healthcare. Activities not related to the present article: none to disclose. Other relationships: receives royalties from a patent for MR fingerprinting licensed to Siemens Healthcare. **Y.J.** Activities related to the present article: received a grant from Siemens Healthcare. Activities not related to the present article: none to disclose. Other relationships: receives royalties from a patent for MR fingerprinting licensed to Siemens Healthcare. **S.P.** Activities related to the present article: received a grant from Siemens Healthcare. Activities not related to the present article: none to disclose. Other relationships: receives royalties from a patent for MR fingerprinting licensed to Siemens Healthcare. **L.L.** Activities related to the present article: received a grant from Siemens Healthcare. Activities not related to the present article: none to disclose. Other relationships: none to disclose. **M.D.T.** Activities related to the present article: received a grant from Siemens Healthcare. Activities not related to the present article: none to disclose. Other relationships: none to disclose. **K.L.W.** Activities related to the present article: received a grant from Siemens Healthcare. Activities not related to the present article: none to disclose. Other relationships: receives royalties from a patent for MR fingerprinting licensed to Siemens Healthcare. **N.S.** Activities related to the present article: received a grant from Siemens Healthcare. Activities not related to the present article: none to disclose. Other relationships: receives royalties from a patent for MR fingerprinting licensed to Siemens Healthcare. **M.A.G.** Activities related to the present article: received a grant from Siemens Healthcare. Activities not related to the present article: none to disclose. Other relationships: receives royalties from a patent for MR fingerprinting licensed to Siemens Healthcare. **V.G.** Activities related to the present article: received a grant from Siemens Healthcare. Activities not related to the present article: none to disclose. Other relationships: receives royalties from a patent for MR fingerprinting licensed to Siemens Healthcare.

## References

- Kim KA, Park MS, Kim IS, et al. Quantitative evaluation of liver cirrhosis using  $T_1$  relaxation time with 3 tesla MRI before and after oxygen inhalation. *J Magn Reson Imaging* 2012;36(2):405–410.
- Huang Y, Sadowski EA, Artz NS, et al. Measurement and comparison of  $T_1$  relaxation times in native and transplanted kidney cor-



- tex and medulla. *J Magn Reson Imaging* 2011; 33(5):1241–1247.
3. Fenlon HM, Tello R, deCarvalho VL, Yucel EK. Signal characteristics of focal liver lesions on double echo T2-weighted conventional spin echo MRI: observer performance versus quantitative measurements of T2 relaxation times. *J Comput Assist Tomogr* 2000;24(2):204–211.
  4. Tello R, Fenlon HM, Gagliano T, deCarvalho VL, Yucel EK. Prediction rule for characterization of hepatic lesions revealed on MR imaging: estimation of malignancy. *AJR Am J Roentgenol* 2001;176(4):879–884.
  5. Goldberg MA, Hahn PF, Saini S, et al. Value of T1 and T2 relaxation times from echoplanar MR imaging in the characterization of focal hepatic lesions. *AJR Am J Roentgenol* 1993;160(5):1011–1017.
  6. Jamin Y, Tucker ER, Poon E, et al. Evaluation of clinically translatable MR imaging biomarkers of therapeutic response in the TH-MYC transgenic mouse model of neuroblastoma. *Radiology* 2013;266(1):130–140.
  7. Weidensteiner C, Allegrini PR, Sticker-Jantschkeff M, Romanet V, Ferretti S, McSheehy PM. Tumour T1 changes in vivo are highly predictive of response to chemotherapy and reflect the number of viable tumour cells: a preclinical MR study in mice. *BMC Cancer* 2014;14(1):88.
  8. Ma D, Gulani V, Seiberlich N, et al. Magnetic resonance fingerprinting. *Nature* 2013;495(7440):187–192.
  9. European Society of Radiology (ESR). Magnetic resonance fingerprinting: a promising new approach to obtain standardized imaging biomarkers from MRI. *Insights Imaging* 2015;6(2):163–165.
  10. Jiang Y, Ma D, Seiberlich N, Gulani V, Griswold MA. MR fingerprinting using fast imaging with steady state precession (FISP) with spiral readout. *Magn Reson Med* 2014 Dec 9. [Epub ahead of print]
  11. de Bazelaire CMJ, Duhamel GD, Rofsky NM, Alsop DC. MR imaging relaxation times of abdominal and pelvic tissues measured in vivo at 3.0 T: preliminary results. *Radiology* 2004;230(3):652–659.
  12. Duyn JH, Yang Y, Frank JA, van der Veen JW. Simple correction method for k-space trajectory deviations in MRI. *J Magn Reson* 1998;132(1):150–153.
  13. Sacolick LI, Wiesinger F, Hancu I, Vogel MW. B1 mapping by Bloch-Siegert shift. *Magn Reson Med* 2010;63(5):1315–1322.
  14. Gao Y, Chen Y, Ma D, et al. Preclinical MR fingerprinting (MRF) at 7 T: effective quantitative imaging for rodent disease models. *NMR Biomed* 2015;28(3):384–394.
  15. Sung K, Daniel BL, Hargreaves BA. Transmit B1+ field inhomogeneity and T1 estimation errors in breast DCE-MRI at 3 tesla. *J Magn Reson Imaging* 2013;38(2):454–459.
  16. Treier R, Steingoetter A, Fried M, Schwizer W, Boesiger P. Optimized and combined T1 and B1 mapping technique for fast and accurate T1 quantification in contrast-enhanced abdominal MRI. *Magn Reson Med* 2007;57(3):568–576.
  17. Chen Y, Lee GR, Aandal G, et al. Rapid volumetric T1 mapping of the abdomen using three-dimensional through-time spiral GRAPPA. *Magn Reson Med* 2015 May 18. [Epub ahead of print]
  18. Stanisz GJ, Odobina EE, Pun J, et al. T1, T2 relaxation and magnetization transfer in tissue at 3T. *Magn Reson Med* 2005; 54(3):507–512.
  19. Brink WM, Gulani V, Webb AG. Clinical applications of dual-channel transmit MRI: A review. *J Magn Reson Imaging* 2015; 42(4):855–869.
  20. Lattanzi R, Sodickson DK, Grant AK, Zhu Y. Electrodynamical constraints on homogeneity and radiofrequency power deposition in multiple coil excitations. *Magn Reson Med* 2009;61(2):315–334.
  21. Gambarota G, Veltien A, van Laarhoven H, et al. Measurements of T1 and T2 relaxation times of colon cancer metastases in rat liver at 7 T. *MAGMA* 2004;17(3-6):281–287.
  22. Raza SA, Funicelli L, Sohaib SA, et al. Assessment of colorectal hepatic metastases by quantitative T2 relaxation time. *Eur J Radiol* 2012;81(4):e536–e540.
  23. Seiberlich N, Lee G, Ehses P, Duerk JL, Glikson R, Griswold M. Improved temporal resolution in cardiac imaging using through-time spiral GRAPPA. *Magn Reson Med* 2011;66(6):1682–1688.
  24. Ye H, Ma D, Jiang Y, et al. Accelerating magnetic resonance fingerprinting (MRF) using t-blipped simultaneous multislice (SMS) acquisition. *Magn Reson Med* 2015 Jun 8. [Epub ahead of print]
  25. Pierre EY, Ma D, Chen Y, Badve C, Griswold MA. Multiscale reconstruction for MR fingerprinting. *Magn Reson Med* 2015 Jun 30. [Epub ahead of print]
  26. Christen T, Pannetier NA, Ni WW, et al. MR vascular fingerprinting: A new approach to compute cerebral blood volume, mean vessel radius, and oxygenation maps in the human brain. *Neuroimage* 2014;89:262–270.
  27. Jiang Y, Ma D, Wright KL, Seiberlich N, Gulani V, Griswold MA. Simultaneous T1, T2, diffusion and proton density quantification with MR fingerprinting [abstr]. In: Proceedings of the Twenty-Second Meeting of the International Society for Magnetic Resonance in Medicine. Berkeley, Calif: International Society for Magnetic Resonance in Medicine, 2014; 28.
  28. Wright KL, Ma D, Jiang Y, Gulani V, Griswold MA, Hernandez-Garcia L. Theoretical framework for MR fingerprinting with ASL: simultaneous quantification of CBF, transit time, and T1 [abstr]. In: Proceedings of the Twenty-Second Meeting of the International Society for Magnetic Resonance in Medicine. Berkeley, Calif: International Society for Magnetic Resonance in Medicine, 2014; 417.